Bulletin of the Seismological Society of America, Vol. 104, No. 4, pp. –, August 2014, doi: 10.1785/0120130142

Ⓔ

Stress Transfer by the 2008 M_w 6.4 Achaia Earthquake to the Western Corinth Gulf and Its Relation with the 2010 Efpalio Sequence, Central Greece

by M. Segou,* W. L. Ellsworth, and T. Parsons

Abstract We investigate the interaction between transform faults and normal faults in western Greece based on seismological analysis and static stress transfer calculations associated with the 8 June 2008 M_w 6.4 Achaia earthquake. We present a relocated earthquake catalog for the period between June 2008 and January 2010, when two normal-faulting events on 18 (M_w 5.3) and 22 (M_w 5.2) January 2010 occurred at Efpalio (western Corinth gulf). They were located approximately 70 km northeast from the buried right-lateral fault, identified as the causative structure of the Achaia earthquake. The first Efpalio event ruptured a mapped normal fault that trends east-northeast–west-southwest, dipping 55°–60° to the south. We estimate ~2-fold seismicity rate changes in the western Corinth gulf region for the interseismic period (June 2008–January 2010), and we find that inside this interval, the monthly event rate remained increased at a 2σ significance level. We calculate a Coulomb stress increase (0.1–0.6 bar) in the Efpalio region using optimally oriented for failure planes, and an ~0.11 bar Coulomb stress increase at the hypocenters of the January 2010 events when incorporating geologically defined receiver planes. We conclude that the positive static stress changes following the Achaia event promoted the observed spatio-temporal clustering in the Corinth gulf for this specific period. We identify fault unclamping due to normal stress reduction as the physical mechanism in this case. The high seismic-hazard character of the target region (0.24g) in the National Building Code emphasizes the importance of time-dependent earthquake probabilities and stress-mediated fault interaction studies.

Online Material: Tables of relocated seismicity and station corrections.

Introduction

On 8 June 2008 at 12:25 UTC, a strong earthquake struck western Greece, activating a buried strike-slip structure, the newly discovered Achaia fault zone (ACFZ). To date, we have no evidence for previous activation of a similar structure in its source region, although historic earthquakes with $\mathbf{M} > 6.0$ have been identified in the broader region (Papazachos and Papazachou, 1989). The causative fault is not evident in the instrumental record (1964–2008; Fig. 1a), which points out the problem of seismic hazard from undiscovered faults. Previous tectonic and geophysical studies have not mapped extensive active strike-slip faults in the area, even though oil exploration studies have noted the complex evolution of the western Peloponnese, with two major deformation phases: a compressional phase, responsible for the north–south fault-and-fold thrust belt, was cut by the latest extensional phase that created the west-northwest–east-southeast-trending normal faults (Kamberis *et al.*, 2000). Focal mechanism and moment tensor solutions support the right-lateral strike-slip character of the ACFZ (Ganas *et al.*, 2009; Konstantinou *et al.*, 2009; Feng *et al.*, 2010; Papadopoulos *et al.*, 2010), which parallels the offshore Cephallonia transform zone (CTZ; Sachpazi *et al.*, 2000) located 150 km to the west (Fig. 1b). The CTZ plays a critical role in the geodynamics of western Greece because it marks the continental collision between the Apulia and Aegean microplates and has slip rates of up to 20 mm/yr (Serpelloni *et al.*, 2005). The ACFZ corresponds to a second-order structure, setting the eastern boundary of the Ionian Islands block (Vassilakis *et al.*, 2011).

In this study, our target region is the continental rift zone of the western Corinth gulf, with well-expressed normal faults (Doutsos and Piper, 1990; Roberts and Koukouvelas, 1996),

*Now at GeoAzur, 250 Rue Einstein, Sophia Antipolis 06560, France.

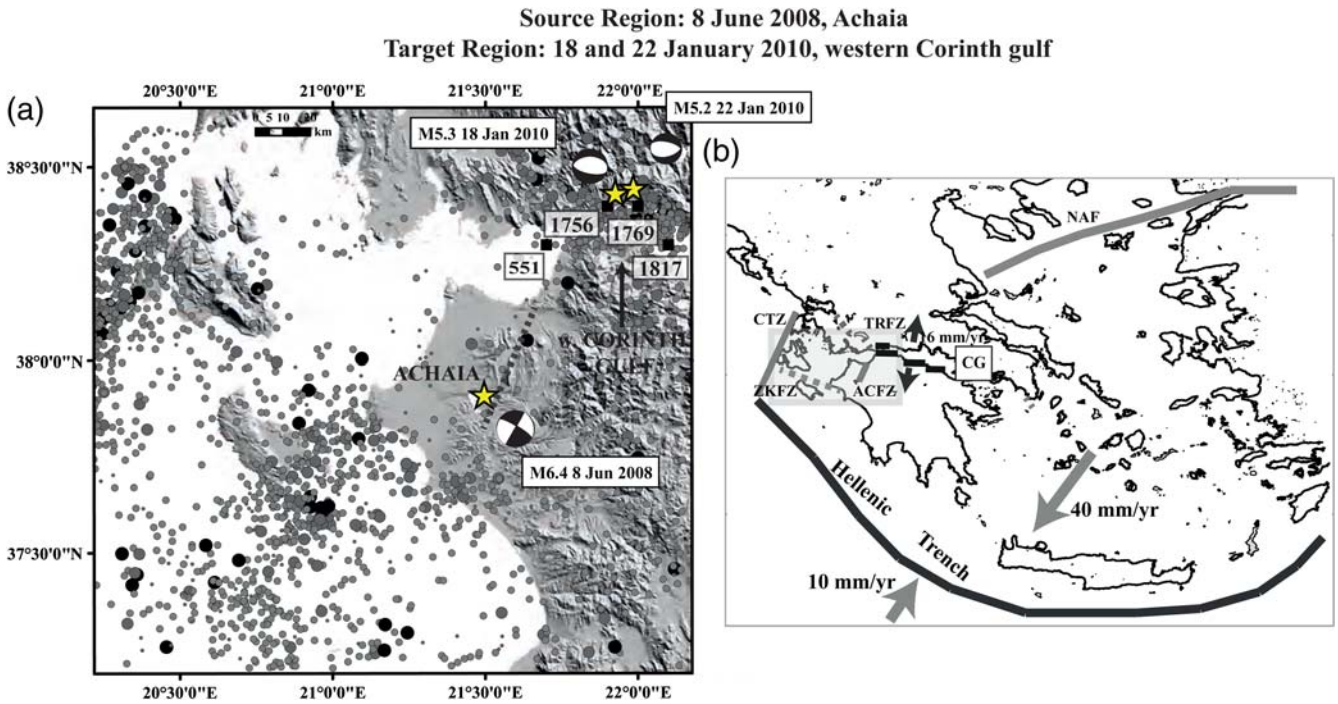

Figure 1. (a) Instrumental seismicity (circles) for the January 1964–June 2008 time period for the western Greece region, taken from the International Seismological Centre (ISC) bulletin. Events with small, gray, large gray, and black circles correspond to magnitudes greater than **M** 3.5, 4.5, and 5.5, respectively. Important historical events (551, 1756, 1769, 1817) with **M** > 6.5 at the target region, western Corinth gulf, are indicated in black squares (taken from Papazachos *et al.*, 2000). The epicenters of the Achaia and Efpalio events are shown with stars. Moment tensor solutions are from the Global Centroid Moment Tensor (Global CMT) database and Sokos *et al.* (2012) for Achaia and Efpalio events, respectively. (b) Locations of the major faults zones inside our study area. The most prominent feature is the Cephallonia transform zone (CTZ), marking the continental collision of Apulia with the Aegean microplate. The left-lateral Zakynthos fault zone (ZKFZ), between western Peloponnese and northern Zakynthos Island, was traced by focal mechanism solutions (Melis *et al.*, 1994). The right-lateral Achaia fault zone (ACFZ) was recognized after the M_w 6.4 June 2008 earthquake and could not be identified in the background seismicity. The left-lateral Trichonis fault zone (TRFZ) lies north of the Corinth gulf (CG). The normal faults trending east–west dominate the continental rift of the Corinth gulf. The geometry at depth of those faults is still a matter of debate; at shallow depths (z < 5 km) inferred dips are about 60°, but the seismological and geodetical analyses following the 1995 M_w 6.4 Aigio sequence supported the existence of a shallow north-dipping surface at 30° (Rigo *et al.*, 1996; Bernard *et al.*, 1997). The color version of this figure is available only in the electronic edition.

extension rates reaching 15–16 mm/yr (Briole *et al.*, 2000; Avallone *et al.*, 2004), and a plethora of strong historic earthquakes (Fig. 1). Following the 2008 Achaia event, the seismicity rate in the target area underwent a statistically significant rate increase. In January 2010, a doublet of two moderate seismic events (M_w 5.3 on 18 January 2010 and M_w 5.2 on 22 January) occurred in the target region near Efpalio village on the northern shore of the gulf at a distance approximately 70 km northeast from the 2008 M_w 6.4 Achaia rupture.

Here, we present static stress-change calculations, taking into consideration such critical parameter choices as source and receiver uncertainties, friction values, and the ambient regional stress field following the 2008 Achaia event. We explore mechanisms for stress-mediated seismicity rate changes in our target region and investigate the hypothesis that the Achaia rupture promoted the January 2010 Efpalio doublet. The statistical assessment of seismicity rate changes involves establishing a magnitude of completeness, together with its time dependence, and a long-term mean background rate for our target region.

Data

We collected earthquake catalogs from a variety of sources for this study: (1) the instrumental catalog of the International Seismological Centre (ISC); (2) *P*- and *S*-wave arrival data from the Hellenic Unified Seismic Network (HUSN; available through the ISC website; see Data and Resources) to relocate earthquakes occurring between June 2008 and January 2010; (3) the historical and noninstrumental catalog between 550 B.C. and 1964 from the Aristotle University of Thessaloniki (Papazachos *et al.*, 2000); and (4) the National Observatory of Athens earthquake catalog for the period after 2000. When our static stress change calculation required knowledge of the local stress field (King *et al.*, 1994), we used a maximum horizontal stress axis at N278°E (Konstantinou *et al.*, 2011).

Observations

Achaia and Efpalio Source Parameters

Source Region. The M_w 6.4 Achaia event occurred on 8 June 2008 12:25:28 UTC on a previously unknown fault

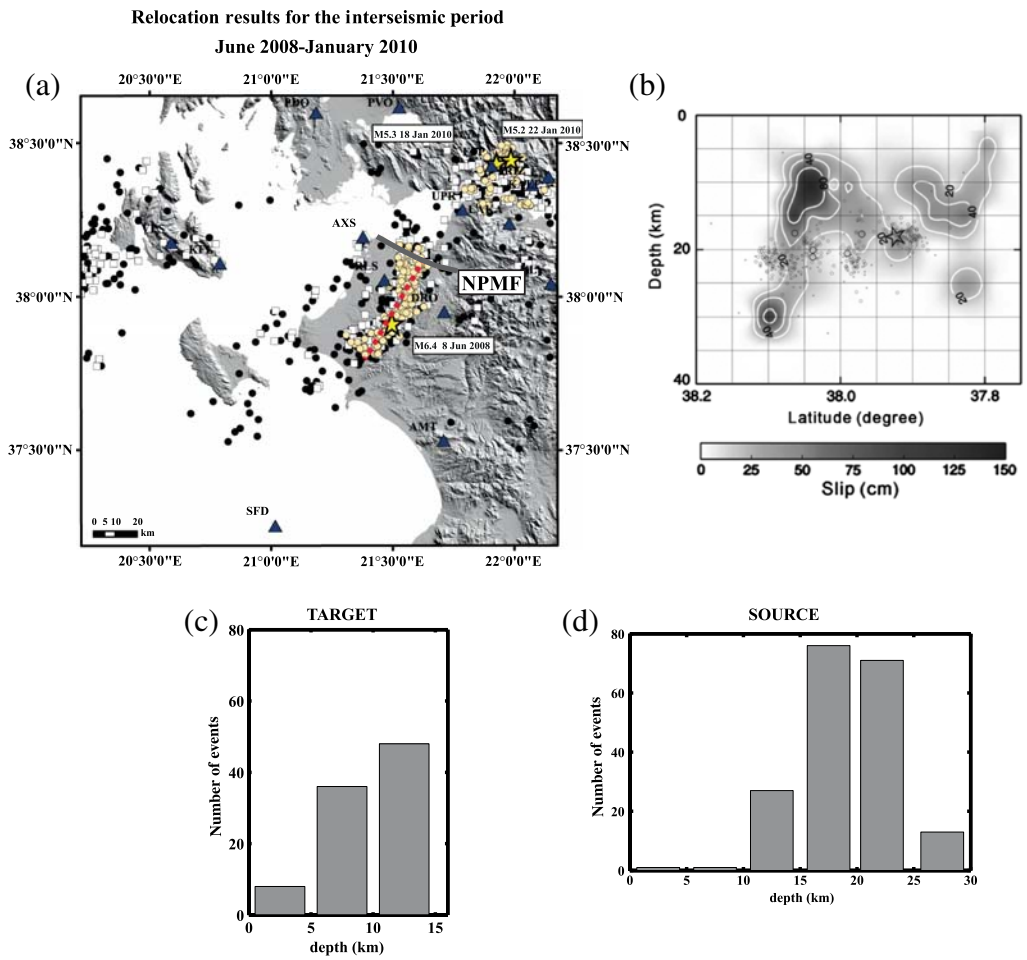

Figure 2. (a) Epicenters for the interseismic period between the **M** 6.4 Achaia and the 30 January 2010 events (mainshocks denoted as stars), including the 18 (M_w 5.3) and 22 (M_w 5.2) January Efpalio events taken from the ISC catalog (in black circles), after joint inversion for hypocenters and 1D velocity model determination using VELEST software (white squares) and the final relocation based on differential travel times using hypoDD (black circles). The inferred causative fault trace is shown as a dashed line. (b) Variable slip-source model by Konstantinou *et al.* (2009); the relocated hypocenter is indicated with a star, and the open circles indicate the relocated aftershocks. (c) and (d) Depth histograms for our target and source regions. The average depths for the source and the target regions are 20 and ~10 km, respectively. The color version of this figure is available only in the electronic edition.

with no surface expression. It nucleated at a depth of 21.4 km (this study) on a vertical strike-slip plane trending N30°E (Fig. 2a). The hypocentral depths of the relocated aftershocks and slip distribution from Konstantinou *et al.* (2009) indicate a mid-to-lower crustal event (Fig. 2d). We use the Konstantinou *et al.* (2009) slip distribution to model the effects of the Achaia event in the target region. It features a large slip patch (maximum slip ~150 cm) between 7 and 20 km depth at the northeast end of the fault. Relocated aftershocks concentrate along the bottom of the slip patch.

Target Region. The Efpalio normal-faulting doublet began with an M_w 5.3 earthquake on 18 January 2010 and was followed 4.5 days after by an M_w 5.2 on 22 January at a distance 5 km to the northeast. The first event is possibly related with the Efpalio fault, which is a prominent south-dipping normal fault on the northern coast of the west Corinth gulf (Gallousi and Koukouvelas, 2007). The second event is correlated with a north-dipping structure (Sokos *et al.*, 2012).

Seismic Event Relocation during the Interseismic Phase (June 2008–January 2010)

We relocated the catalog seismicity for the period between 8 June 2008 and 30 January 2010 to verify that the aftershocks of the Achaia event did not propagate into the target region, which could jeopardize our conclusion regarding the increased seismicity rates discussed in the following paragraph. We consider 501 initial locations with 8 and 5 average *P*- and *S*-wave arrivals, respectively. Our relocation is performed in two consecutive stages: the first one (341 relocated events) is based on the joint inversion for the 1D determination of the velocity structure and hypocenters (Kissling *et al.*, 1994), and these results are used in the second stage (281 relocated events), which utilizes the double-difference

Table 1
Crustal Models Used in This Study

This Study			Makris		Rigo		Latorre			
z (km) *	P-Wave Velocity (km/s)	S Wave	z (km)	P-Wave Velocity (km/s)	z (km)	P-Wave Velocity (km/s)	z (km)	P-Wave Velocity (km/s)	z (km)	P-Wave Velocity (km/s)
0.0	3.86	2.65	0.0	4.00	0.00	4.80	0.00	4.27	6.50	5.83
2.0	5.65	2.86	2.0	5.80	4.00	5.20	2.90	5.06	7.00	6.08
5.0	6.00	3.38	5.0	6.00	7.20	5.80	3.80	5.15	7.70	6.08
15.0	6.43	3.47	15.0	6.25	8.20	6.10	4.50	5.21	8.30	6.35
30.0	7.34	4.09	20.0	6.50	10.40	6.30	5.00	5.35	9.10	6.40
			30.0	7.60	15.00	6.50	6.00	5.53	16.00	6.60
					30.00	7.00	6.50	5.65	33.00	8.37

The Rigo *et al.* (1996) model has been extensively used in the Corinth gulf, and the Latorre *et al.* (2004) model has been more recently proposed for the western Corinth gulf at the proximity of the Efpalio area. For the Makris (1978), Rigo *et al.* (1996), and Latorre *et al.* (2004) models, the S-wave velocity is assumed to be $1/\sqrt{3}$ of the P-wave speed.

*Depth to top of the layer.

technique based on differential travel times (Waldhauser and Ellsworth, 2000; Waldhauser, 2001). Initial hypocenters, together with the relocated events after joint inversion for hypocenters and the 1D velocity model and the hypoDD analysis, are shown in Figure 2.

We first invert for hypocenters, a 1D velocity model, and station corrections by the computer program VELEST (Kissling *et al.*, 1994), using 5422 and 3386 P- and S-wave phases, respectively. The starting velocity model for the event relocation (Makris, 1978) has six layers (Table 1). The reason for testing the initial velocity model is to confirm the lower crustal nature of Achaia sequence, which is somewhat atypical of the seismicity of the region. We randomly select two groups of 50 events and extensively test the effect of the weighting factor for S relative to P arrivals and the influence of initial hypocentral locations (using fixed depth at 6 and 12 km), the thickness, and the upper boundary of the lower crustal layer (using 6, 10, 12, 15, 18, and 20 km as possible upper boundaries). The preferred velocity model presents a single layer between 15 and 30 km (Table 1). Ⓔ The root mean square (rms) residuals decrease from 0.42 to 0.20 s after 21 iterations, presented analytically in Figure S1, available in the electronic supplement to this article.

At the second step, we used hypoDD software (Waldhauser and Ellsworth, 2000) to achieve better hypocenter locations, based on travel-time differences for pairs of earthquakes at common stations. The first step involved analysis of the arrival-phase data to derive travel-time differences for paired earthquakes. We adopt the typical definition of a strong link (Waldhauser, 2001), including at least eight phase pairs with a separation distance less than 10 km. Original phases were weighted equally, although a reweighting scheme was imposed at each of the four iteration steps per inversion, based on varying the weight of S-wave phases relative to P wave (0.10, 0.20, 0.25, and 0.50), and different damping factors (10, 20, and 40). In Ⓔ Figure S2, we present the rms reduction after each of the 24 iterations, resulting in our final relocation in average rms 0.19 s. Although the least-squares conjugate gradients method (LSQR) is efficient in relocating large datasets, it is important to assess the hypocenter uncertainties through the singular-value decomposition (SVD) method (Waldhauser, 2001). In this study, we test the stability of the LSQR solution by applying the SVD solver in a subset of 150 randomly selected events. Ⓔ To illustrate a comparison between the results derived by each solver, we present a map view of epicenter locations and histograms of rms residuals in Figure S3. Based on the analysis of the subset of data with the SVD method, the average uncertainty in the new locations is 0.57 km in the east–west direction, 0.96 in the north–south direction, and 1.1 km in the vertical direction. We have also investigated the effect of variation in the initial locations on the hypoDD solution by using either catalog data or the cluster centroid. Ⓔ Similar to the previous illustration, we present our results in map view and in rms histograms in Figure S4. However, at our final relocation we support the use of catalog data, corresponding to the output of the early relocation stage through VELEST code, as initial locations for the double-different (DD) method because the centroid option is "appropriate for clusters of small dimensions" (Waldhauser, 2001). In Figure 3, we present relocation results for the source and the target region, respectively.

We perform an additional test for our relocation results within our target region, the western Corinth gulf area, comparing the Rigo *et al.* (1996), Latorre *et al.* (2004), and the preferred velocity model (Table 1). We assess the uncertainty of the relocated hypocenters for the two January 2010 mainshocks and four other events in their vicinity, having more than 25 phase arrivals, using the aforementioned models. We use the DD locations as input for the VELEST code, and we redetermine their hypocenters without allowing the velocity model to vary. We find that the Latorre *et al.* (2004) model yields shallower hypocenters (average rms = 0.23; average depth = 4 km), whereas our model results in deeper hypocenters (average depth = 8 km) with reduced average rms = 0.21 and the Rigo *et al.* (1996) model had an intermediate depth approximation with an average depth

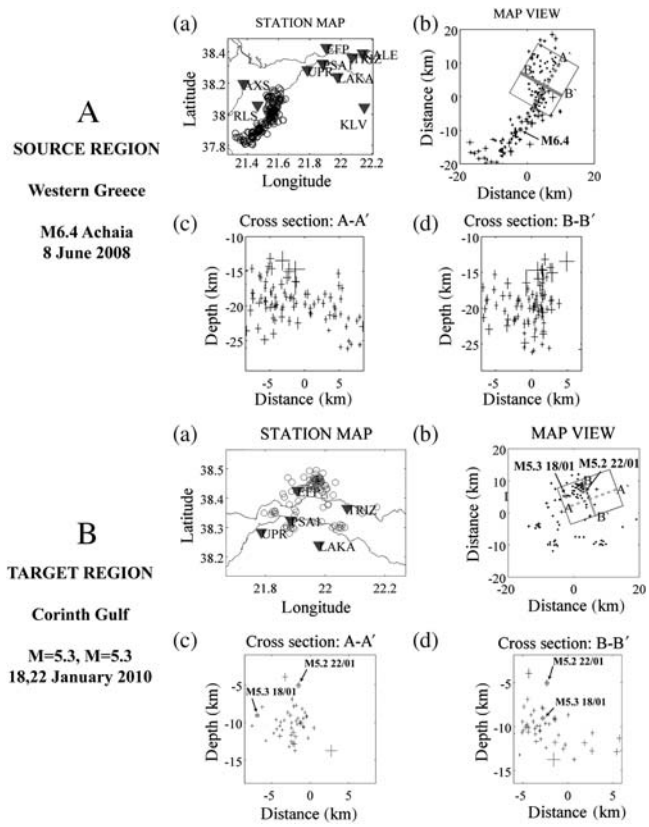

Figure 3. Panels A (above) and B (below) present relocation results for the source and the target region, respectively. In each panel, (a) and (b) show the local station together with the relocation results in map view, and (c) and (d) show cross-sections along strike and perpendicular to the ACFZ (panel A) and Efpalio fault (panel B).

of 6 km and rms = 0.23. When considering these, we conclude that the estimated velocity model of this study should be used in the final hypocenter determination, but we admit that the difference with the other models is small. The main difference between the preferred one and the other models is the lower velocity near the surface. Ⓔ The catalog of relocated events is provided in Table S1, together with the station corrections in Table S2; the relocation of Achaia and Efpalio events are presented in Table 2.

By assessing the relocated events, we find that aftershocks of the Achaia rupture did not propagate northeast toward the Efpalio sequence, which might have provided an alternative explanation to static stress transfer for the increased seismicity rates in the western Corinth gulf. Our relocation results indicate that the northern extent of the Achaia rupture was bounded by an inactive low-angle normal fault (NPMF in Fig. 2) that crosscuts the northern Peloponnese (Flotté *et al.*, 2005).

Static Stress-Change Modeling

Testing the hypothesis that the Achaia event triggered earthquakes in the western Corinth gulf and promoted the Efpalio events by static stress transfer involves a number of free parameters, such as the coseismic slip distribution, the friction coefficient and the geometry of receiver faults, and the ambient stress field orientation. We first investigate the effect of stress changes in our target region by estimating the observed seismicity rate changes at distances > 30 km from the rupture plane to ensure that no direct aftershock of the Achaia event is included. Second, we explore whether the Achaia event has promoted the occurrence of the Efpalio doublet, focusing on the 18 January event.

Table 2
Seismic Parameters of the Mainshocks

Event Date (yyyy/mm/dd)	Event Time (hh:mm:ss.ss)	Latitude (°)	Longitude (°)	Depth (km)
2008/06/08	12:25:28.01	37.91	21.49	21.35
2010/01/18	15:56:08.02	38.43	21.92	9.03
2010/01/22	00:46:55.11	38.44	21.98	5.05

The Coulomb failure criterion was implemented as follows:

$$\Delta\tau = |\Delta\bar{\tau}_f| + \mu(\Delta\sigma_n + \Delta_p), \quad (1)$$

in which $|\Delta\bar{\tau}_f|$ is the shear stress change parallel to the receiver fault rake, μ is the friction coefficient, $\Delta\sigma_n$ is the stress change normal to the fault plane, and Δ_p is the pore pressure change. We account for pore fluid pressure effects by using the effective coefficient of friction, which assumes a Skempton coefficient B_k so that $\mu' = \mu(1 + B_k)$, and the Coulomb criterion, following Rice (1992) formulation, is given by

$$\Delta_\tau = |\Delta\tau_f| + \mu'(\Delta\sigma_n). \quad (2)$$

Before we investigate the correlation between static stress changes and observed seismicity, we check the stability of our calculations by varying several critical free parameters in Figure 4. We explore pore fluid pressure effects by assuming effective friction to take values between 0.0 and 0.8. We demonstrate the stability of our optimally oriented failure plane stress calculations by considering a range of apparent friction coefficient values ($\mu' = 0.2$, 0.4, 0.6, and 0.8; Fig. 4a–d), receiver depths ($z = 10$ and 20 km; Fig. 4b–e), and regional stress field orientations (Fig. 4f). We note that using a shallow target depth ($z = 10$ km) causes an increased localized positive Coulomb stress change by 5 bars (Fig. 4), related to the high-slip patch 15 km northeast from the epicenter at approximately 12 km depth (Fig. 2b). For clarification purposes, we point out that the friction values related to stress-change calculations in this article refer to apparent friction coefficient values. We do not observe significant differences when considering the above parameters, and we therefore conclude that the static stress-change calculations through the seismogenic crust are not very sensitive to friction coefficient and depth variation.

Concerning the ambient stress field, we take a maximum horizontal compression axis of N273°E, derived after focal mechanism inversion from 21 events with **M** > 3.5 prior to

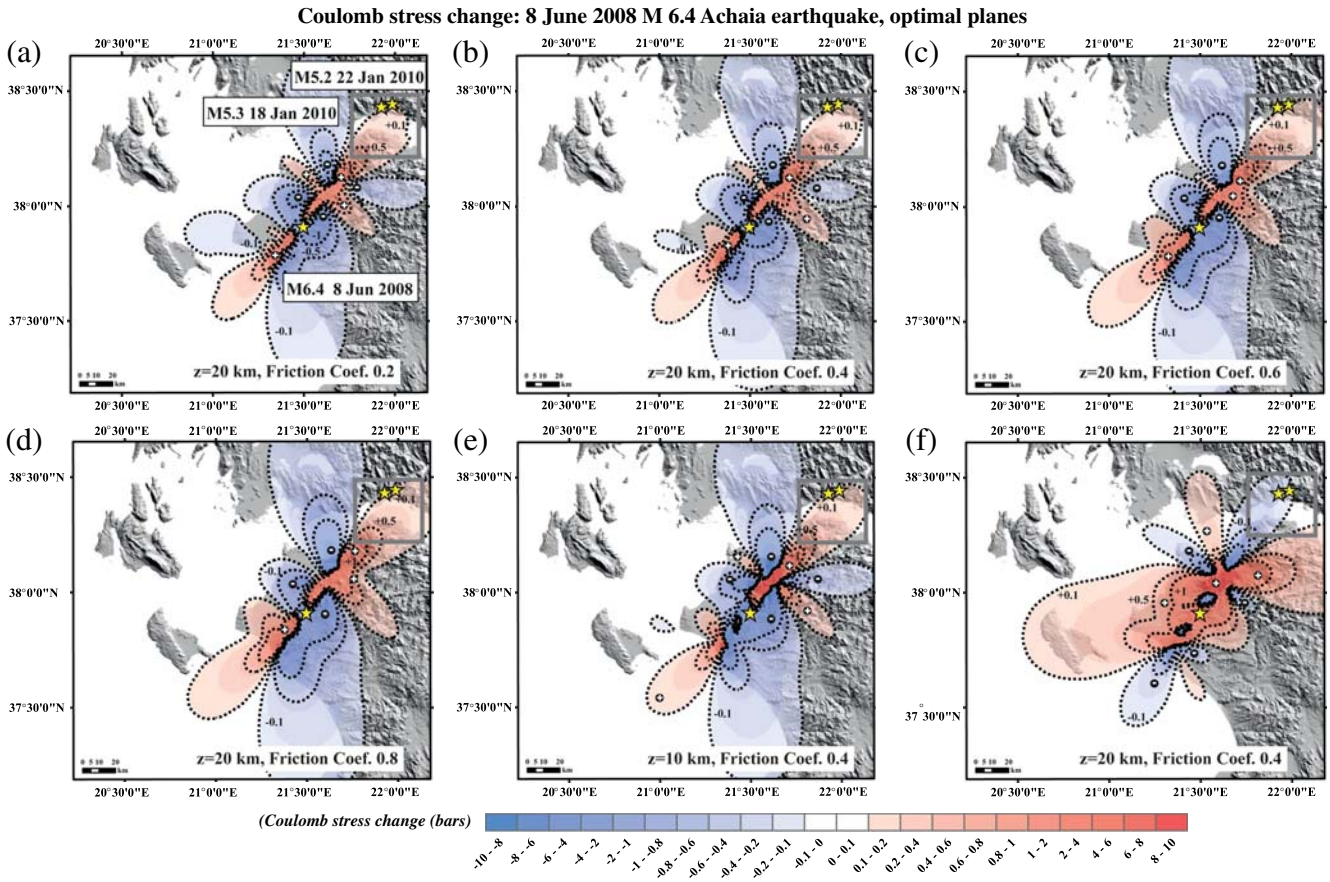

Figure 4. Coulomb stress changes imparted by the right-lateral Achaia **M** 6.4 event that occurred on 8 June 2008, resolved on optimally oriented for failure planes. (a–d) We examine the sensitivity of Coulomb static stress-change calculations to varying values of friction coefficient for target depth 20 km, (e) for friction coefficient $\mu' = 0.4$ for target depth at 10 km, and (f) friction coefficient $\mu' = 0.4$ for target depth at 20 km. We have used the variable-slip model of Konstantinou *et al.* (2009) throughout our calculations for our source representation of the Achaia event, whereas stress changes were resolved on optimally oriented for failure planes (King *et al.*, 1994). We note that in (a–e), the regional stress field is represented by the typical σ_1–σ_3 orientation, derived from stress inversion of Konstantinou *et al.* (2011), giving a maximum horizontal axis at 273° with $[\sigma_1, \sigma_2, \sigma_3] = [100, 10, 0]$, whereas in (f) the principal stresses were taken from the axes in the Global CMT solution for the Achaia event. There is no important variability within the same stress field representation (a–e), whereas in (f) the stress-change pattern differs from the one in (b) due to the significant deviation between *P–B–T* axes and the typical σ_1–σ_3 of the regional stress field, anticipated for major faults at the vicinity of plate boundaries (Heidback *et al.*, 2010). The color version of this figure is available only in the electronic edition.

the Achaia shock (Konstantinou *et al.*, 2011). Because of limited information regarding the absolute magnitude of principal stresses in our region, we have applied a simplified case of regional compression of 100 bars and $\sigma_2 = 10$ bars. Worldwide *in situ* measurements of stress magnitude can be conducted by hydraulic fracturing, overcoring, and well-core breakouts (e.g., Zoback and Magee, 1991) or *P*- and *T*-axes analysis of off-fault earthquake focal mechanism data (e.g., Hardebeck and Michael, 2004). We furthermore compare these with the principal *P–B–T* axes of the Global Centroid Moment Tensor (Global CMT) of the mainshock. Generally, *P–B–T* axes can be a good approximation of the principal stress orientations with the exception of locations at the vicinity of plate boundary zones, because in those areas they are related with differences in the mechanical properties along major faults (Heidbach *et al.*, 2010). This fact, along with Figure 4f, provides further evidence that ACFZ is at a high angle to the stress field, implying that the Achaia fault is not optimally oriented for failure, a conclusion that was also supported by previous studies (Konstantinou *et al.*, 2011).

Increased Seismicity Rates in the Corinth Gulf

We observe in Figure 5 that the post-Achaia shock seismicity in our target region corresponds with the off-fault positive lobe of Coulomb stress changes, with values ranging from a maximum of 0.64 bar (±0.1) and minimum of 0.10 bar (±0.012), when considering varying apparent friction coefficients ($\mu' = 0.2$, 0.4, 0.6, and 0.8). This range results from varying the coefficient of friction for optimally oriented faults at a depth of $z = 10$ km. Coulomb stress-change values are calculated to be greater than 0.1 bar over the target region, which commonly has been identified as a stress threshold for initiating failure (Reasenberg and Simpson, 1992; Hardebeck *et al.*, 1998). Similar to Figure 5,

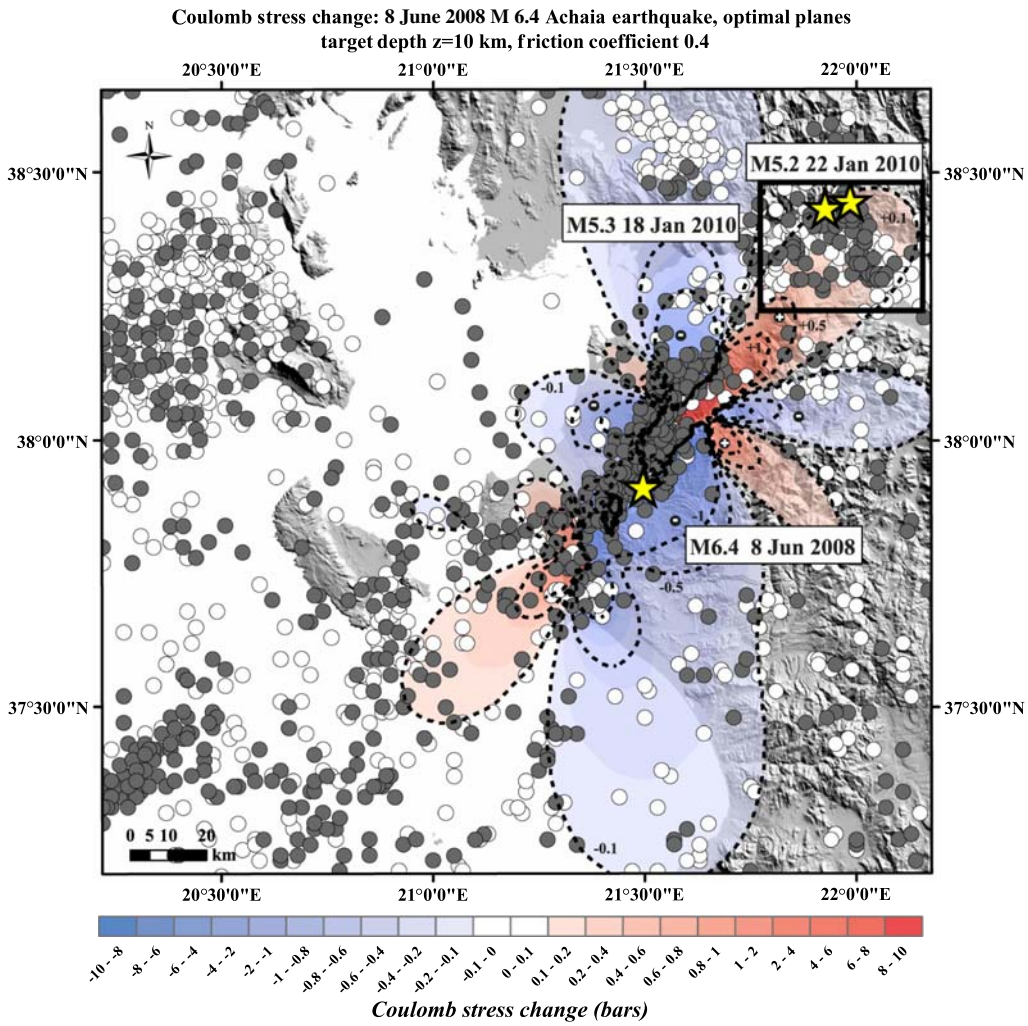

Figure 5. Coulomb static stress change produced by the **M** 6.4 Achaia event of 8 June 2008, resolved on optimally oriented for failure planes (King *et al.*, 1994) at target depth $z = 10$ km with a friction coefficient value $\mu' = 0.4$. We use the variable slip-source model from Konstantinou *et al.* (2009) and a maximum compressive horizontal axis at 273° (Konstantinou *et al.*, 2011) with $[\sigma_1, \sigma_2, \sigma_3] = [100, 10, 0]$. Our goal is to examine whether the positive Coulomb static stress changes after the Achaia shock cause a seismicity rate change with the same sign in our target region at the western Corinth gulf (black rectangle). We show earthquake locations with $M_c = 3.2$ for ~1.5 years before (white circles) and after (gray circles) the Achaia event, taken from the catalog of the National Observatory of Athens (mainshocks denoted as stars). The color version of this figure is available only in the electronic edition.

Ⓔ Figure S5a shows the Coulomb stress changes resolved on optimally oriented normal faults, because our target region is an extensional one, and compared with the available CMT solutions for events within the interseismic period provided by the National Observatory of Athens CMT catalog. We observe a very good agreement between the three estimated focal planes (**M** 4.3 7 June 2009, **M** 4.0 3 September 2009, and the Efpalio event **M** 5.3 18 January 2010), the active bounding normal faults (see Fig. 1) and the calculated optimally oriented normal faults within our target region; however, we admit to a limited CMT sample. Ⓔ Furthermore, the panel of figures presented in Figure S5 aims to illustrate the sensitivity of Coulomb stress changes to different magnitudes of the principal stresses; ideally, a successful ambient stress field should promote faulting across all the active faults within our target region. We present a range of stress regimes evolving from extensional strike slip (Ⓔ $R' = 1.1$ in Fig. S5a), to a strike slip with extension features ($R' = 1.23$), and to almost pure strike slip ($R' = 1.34$). We note that the index R' (Delvaux *et al.*, 1997) numerically expresses the stress regime progressing from 0.5 for pure extension, to 1 (extensional strike slip), 1.5 (pure strike slip), 2.0 (strike-slip compressional), and 2.5 for pure compression. In this study, we explore the range between $R' = 1.0$ and 1.5 (extensional strike slip to almost pure strike slip), and Ⓔ we show in Figure S5a–c that normal faulting in an east–west direction in the western Corinth gulf is promoted by the stress changes following the rupture of the ~30° N ACFZ under different assumptions for the magnitude of principal stresses for the ambient stress field.

When making rate-change calculations, it is necessary to take into consideration how the completeness magnitude

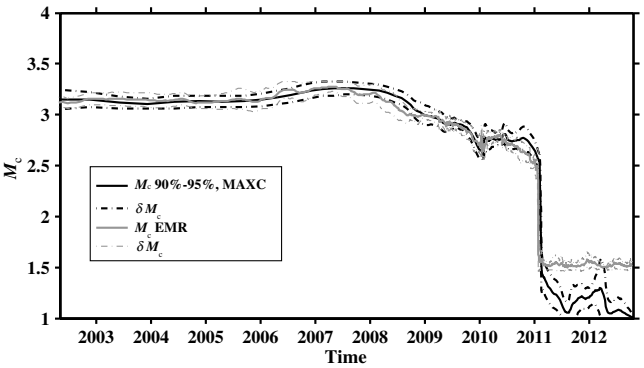

Figure 6. Time-dependent estimation of M_c at 95% confidence level for the 2000–2012 time period inside the target area outline by the black rectangle in Figure 5. We determined the maximum completeness magnitude, $M_c = 3.2$, corresponding to the time period between before the change to modern instrumentation within the Hellenic Unified Seismic Network (mid-2008) and the occurrence of the **M** 6.4 Achaia earthquake.

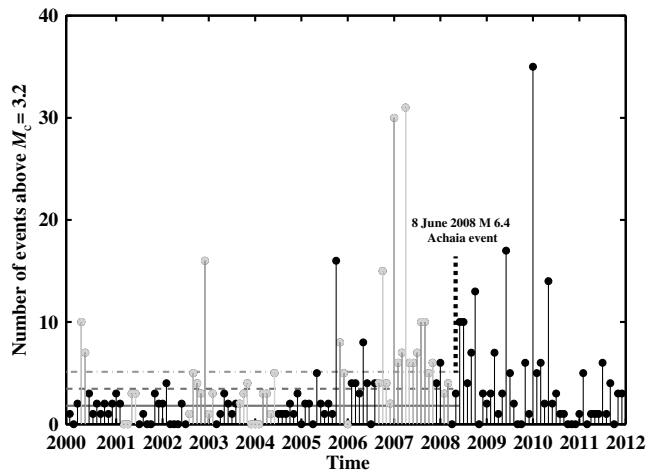

Figure 7. Monthly seismicity rate for the 2000–2012 time period above the $M_c = 3.2$ inside the target area. In the process of estimating the mean seismicity rate, we excluded the well-documented swarm periods found in recent scientific literature (Orfanogiannaki and Papadopoulos, 2004; Kapetanidis, 2007; Kapetanidis *et al.*, 2008; Borouis and Cornet, 2009; Pacchiani and Lyon-Caen, 2010) for the western Corinth gulf (event rates with these events included are shown in gray). Horizontal solid, dashed, and dotted-dashed lines correspond to the mean monthly event rate, mean $+1\sigma$, and mean $+2\sigma$, respectively, for the time period before the 2008 Achaia event. We observe that the monthly seismicity rates following the **M** 6.4 Achaia event exceed the $+1\sigma$ level up to the occurrence of the Efpalio 18 January event.

of the earthquake catalog changed inside our target region during the 2000 and 2011 period. In Figure 6, we present the $M_c = f(t)$, in which M_c is either the best combination among the 90%–95% of confidence levels and the frequency–magnitude distribution maximum curvature method (Wiemer and Wyss, 2000) or is estimated by the entire-magnitude-range (EMR) method. To create the time series of M_c, we chose a moving window of 350 events (window overlap = 100 events, minimum sample size 50 events), with a 0.1 **M** binning and uncertainty calculation through 250 bootstraps (Wiemer, 2001). We estimate a maximum (poorest) $M_c = 3.2$ for the period between 2007 and mid-2008, which we further adopt as a counting threshold. We consider the estimated magnitude of completeness robust, because it was confirmed further by the EMR method, which according to Woessner and Wiemer (2005) is the most favorable choice for M_c determination (Ⓔ Fig. S6). The recent reduction of M_c reflects the many improvements that have occurred since the HUSN was established in mid-2008.

In Figure 7, we present the monthly count of $M_c \geq 3.2$ earthquakes inside our target region since 2000. We apply the β-statistic of Matthews and Reasenberg (1988) to determine if the rate changed following the 2008 Achaia earthquake. We estimate that the mean monthly rate, starting in January 2000 and ending before the 2008 Achaia event, is 1.8 ± 1.6. Immediately after the 2008 Achaia event, the monthly rates lie above the $+2\sigma$ level for the following 6 months and stay above the $+1\sigma$ level for 12 months in the interseismic period between the Achaia and the Efpalio events. We excluded periods that have been identified as swarm episodes related to fluid circulation (light gray in Fig. 6) (Orfanogiannaki and Papadopoulos, 2004; Kapetanidis, 2007; Kapetanidis *et al.*, 2008; Borouis and Cornet, 2009; Pacchiani and Lyon-Caen, 2010) from our mean background rate calculations because the artificial high background rates would lead to biased rate-change calculations for the post-Achaia shock time period.

Is It Likely that the Achaia Shock Promoted the Occurrence of the Efpalio Sequence?

After establishing the effects of the static stress changes on local seismicity in our target area, we examine whether the Achaia earthquake promoted the nucleation of the January 2010 Efpalio events. To estimate the static stress changes at the hypocenter of the 18 January Efpalio event, we consider fault plane geometry determined from active fault mapping and moment tensor solutions (Table 3). We observe that the hypocenter of the 18 January event was subject to an increased Coulomb stress of 0.08–0.10 bar, with shear and normal stress increases of 0.05 and 0.09 bar, respectively. At the hypocenter of the second Efpalio event of 22 January, the calculated Coulomb stress increases vary between 0.09 and 0.11 bar; however, the nucleation of this event might have been strongly influenced by other phenomena (postseismic relaxation, secondary triggering). We identified 10 events during the interseismic phase that have $\mathbf{M} > 3.8$ within a 10 km distance from the epicenter of the 18 January event.

The static stress-change calculations are shown in Figure 8a–c, resolved on specific receiver faults based on geological data corresponding to the Efpalio fault. Figure 8a presents the Coulomb stress changes for an apparent friction coefficient $\mu' = 0.4$ and selected contours at ± 0.1, 0.5, and 1.0 bars for apparent friction coefficients of $\mu' = 0.2$, 0.4, 0.6, and 0.8. Coulomb stress changes are calculated to be higher than 0.1 bar at both the 18 and 22 January epicenters for friction values of $\mu \geq 0.4$. Figure 8b shows that shear stress

Table 3
Static Stress-Change Calculations at the Hypocenters of the 18 and 22 January 2010 Events

Event (yyyy/mm/dd)	Receiver Geometry: Strike/Dip/Rake (°)	Target Depth (km)	Static-Stress Changes (bars)		
			Coulomb	Shear	Normal
2010/01/18	$P_1 : 80/60/-90$	9.03	0.10 (±0.02)	0.05	0.09
2010/01/18	$P_2 : 270/36/-100$	6.6	0.08 (±0.01)	0.05	0.05
2010/01/22	$P_1 : 80/60/-90$	5.05	0.11 (±0.02)	0.06	0.10
2010/01/22	$P_2 : 78/40/-109$	8.0	0.09 (±0.01)	0.07	0.06

The receiver geometry P_1 and P_2 is defined from active fault mapping (e.g., Gallousi and Koukouvelas, 2007) and regional moment tensor solutions (supported in Sokos *et al.*, 2012), respectively. The source model was taken from Konstantinou *et al.* (2009). The Coulomb column refers to the mean value of the Coulomb stress change when considering varying friction coefficients ($\mu' = 0.2$, 0.4, 0.6, and 0.8). We considered the hypocentral depths from our relocation for the P_1 case and the ones reported in Sokos *et al.* (2012) for P_2.

changes are also calculated to have increased by ~0.05 bar at the hypocenter of the first Efpalio event. Figure 8c demonstrates positive normal stress changes, denoting fault unclamping of ~0.1 bar at the hypocenter of the 18 January Efpalio event and reaching 0.2–0.25 bar in the broader area. This suggests that the activation of the right-lateral ACFZ unclamped the normal faults in the Corinth gulf.

The strongest modern seismic event (1995 M_w 6.4 Aigio earthquake) on the north coast of the western Corinth gulf is thought to have occurred on a low angle, north-dipping normal fault (Rigo *et al.*, 1996; Bernard *et al.*, 1997). We therefore examine the normal stress changes resolved on the alternative causative fault for the 18 January 2010 event, the east–west striking Psathopirgos fault that dips 30° to the north (Fig. 8d). If we assume that the static stress hypothesis is correct, the magnitude ($\Delta_{n,max} \sim 0.027$ bar) and the spatial distribution of normal stress changes clearly do not favor the latter interpretation.

Generally, fault weakening is attributed to the existence of low-strength materials, high pore pressure lowering normal stress, or interaction between fault systems (Parsons, 2002). Whether the suggested mechanism, the normal stress reduction, is the only fault-weakening procedure is not clear. The Corinth gulf is sustained in a near-critical state with episodes of swarm activity that are usually attributed to high-pore-pressure fluids (Borouis and Cornet, 2009; Pacchiani and Lyon-Caen, 2010). However, according to Perfettini *et al.* (1999), when examining how the 1988 and 1989 Lake Elsman, California, events (M_w 5.3 and 5.4) promoted the 1989 M_w 6.9 Loma Prieta earthquake, "the limitation on such hypotheses is that we have no direct evidence for such preseismic fluid flow." At this point, we support that a simple stress-change calculation can explain the observations, and more complicated processes, while possible, are not necessary to invoke.

Conclusions

The main conclusions of this study are the following:

1. Seismicity rates increased in the western Corinth gulf at a 2σ significance level following the 2008 Achaia earthquake and remained at elevated rates for an extended period (June 2008–January 2010). This rate change is consistent with the long-term effect of static stress changes found elsewhere (e.g., Freed, 2005).
2. We calculate that the Achaia earthquake increased Coulomb stresses on optimally oriented receiver faults in the western Corinth gulf. In particular, the fault that slipped in the 18 January 2010 Efpalio event was unclamped by the Achaia earthquake. We cannot exclude an alternative or complementary mechanism for the Efpalio sequence related with fluid circulation, known to exist inside western Corinth gulf, although there is no evidence for preseismic fluid flow.
3. Our calculations show that the east–west-trending bounding normal faults of the Corinth gulf are ideally situated to interact with the right-lateral ACFZ. Similar cases of stress interaction and earthquake triggering have been identified by Lin and Stein (2004) between the southern San Andreas fault and nearby thrust faults. Moreover, Zhang *et al.* (2008) showed that strike-slip faults could significantly trigger normal faults during the 1997 Jiashi swarm in the Tarim basin, China. In that context, other strike-slip zones in the vicinity of the gulf, such as the left-lateral Trichonis fault zone (~20 km northwest of the Corinth gulf) should be considered when calculating time-dependent earthquake probabilities for this region. Furthermore, recent work (Durand *et al.*, 2013) indicates that the storm of earthquakes in western Greece during 2008 may have been promoted by the retreat of the African slab, which highlights the importance of re-evaluating earthquake probabilities in inner parts of the Aegean plate (such as the Corinth gulf in this study) in response to large seismic events at the vicinity of the Hellenic trench.

Data and Resources

Stress modeling has been performed using the Coulomb software, available at http://earthquake.usgs.gov/research/modeling/coulomb/ (last accessed February 2013). For the estimation of magnitude of completeness with time, we used the Zmap computer code, available at http://www.seismo.

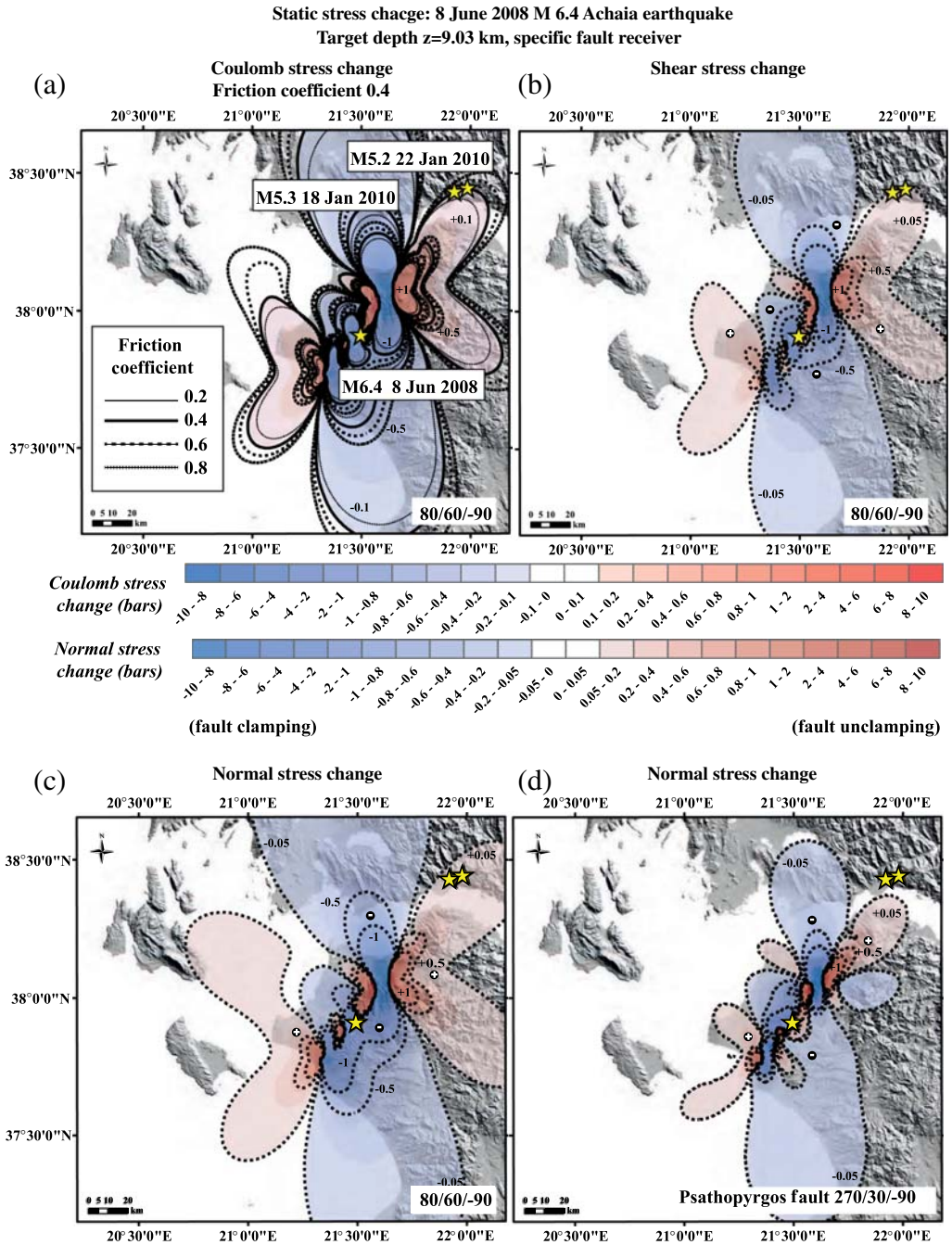

Figure 8. Static stress changes produced by the **M** 6.4 Achaia event of 8 June 2008 adopting the variable slip-source model from Konstantinou *et al.* (2009), resolved on the candidate faults in the target zone (strike/dip/rake of 80°/60°/−90°) at depth $z = 9.03$ km. We present in (a) the Coulomb stress changes for a range of friction coefficient values ($\mu' = 0.2$, 0.4, 0.6, and 0.8), ($\mu' = 0.2, 0.4, 0.6, 0.8$) contoured at ±0.1, 0.5, and 1.0 bar. In (b) and (c), the shear and normal stress changes are contoured at ±0.05, 0.5, and 1.0 bar; note that positive normal stress changes denote fault unclamping. We also consider an alternative geometry (strike/dip/rake of 270°/30°/−90°) for the causative fault of the 18 January 2010 event that corresponds to the Psathopyrgos fault at the southern coast of the gulf, dipping with low angle (30°) to the north. Ⓔ For illustration and clarity purposes, we present panel (a) in greater detail in Figure S6. The color version of this figure is available only in the electronic edition.

ethz.ch/prod/software/zmap/index_EN (last accessed February 2013). For the determination of 1D velocity model from travel-time inversion, we used VELEST software, available upon request from Edi Kissling at iss@tomo.ig.erdw.ethz.ch. For earthquake hypocenter determination through differential travel times, we used hypoDD software, available at http://earthquake.usgs.gov/research/software/ (last accessed February 2013). Preliminary earthquake catalog and phase arrivals for the time period June 2008–January 2010 were recorded at Hellenic Unified Seismic Network (HUSN)

stations and are available through the International Seismic Centre website http://www.isc.ac.uk (last accessed February 2013). Earthquake catalog data before June 2008 is available through the web page of the Geodynamic Institute of the National Observatory of Athens (www.gein.noa.gr/en, last accessed February 2013), as are the moment tensor solutions (http://bbnet.gein.noa.gr/HL/seismicity/moment-tensors, last accessed February 2013). The Global Centroid Moment Tensor Project database was searched using www.globalcmt.org/CMTsearch.html (last accessed February 2013).

Acknowledgments

The authors would like to thank Bob Simpson and Andrea Llenos for their comments and suggestions on an early draft of the manuscript. We also thank Associate Editor Heather DeShon and two anonymous reviewers for their comments and presentation suggestions. The research presented in this paper has been supported by the Earthquake Hazards Program of the U.S. Geological Survey.

References

Avallone, A., P. Briole, A. M. Agatza-Balodimou, H. Billiris, O. Charade, C. Mitsakaki, A. Nercessiana, K. Papazissib, D. Paradissisb, and G. Veis (2004). Analysis of eleven years of deformation measured by GPS in the Corinth Rift Laboratory area, *Compt. Rendus. Geosci.* **336,** no. 4–5, 301–311, doi: 10.1016/j.crte.2003.12.007.

Bernard, P., P. Briole, B. Meyer, H. Lyon-Caen, J.-M. Gomez, C. Tiberi, C. Berge, R. Cattin, D. Hatzfeld, C. Lachet *et al.* (1997). The $M_s = 6.2$, June 15, 1995, Aigion earthquake (Greece): Evidence for low angle normal faulting in the Corinth rift, *J. Seismol.* **1,** 131–150.

Borouis, S., and F. H. Cornet (2009). Microseismic activity and fluid fault interactions: Some results from the Corinth Rift Laboratory (CRL), Greece, *Geophys. J. Int.* **178,** no. 1, 561–580, doi: 10.1111/j.1365-246X.2009.04148.x.

Briole, P., A. Rigo, H. Lyon-Caen, J. C. Ruegg, K. Papazissi, C. Mitsakaki, A. Balodimou, G. Veis, D. Hatzfeld, and A. Deschamps (2000). Active deformation of the Corinth rift, Greece: Results from repeated Global Positioning System surveys between 1990 and 1995, *J. Geophys. Res.* **105,** no. B11, 25,605–25,625, doi: 10.1029/2000JB900148.

Delvaux, D., R. Moeys, G. Stapel, C. Petit, K. Levi, A. Miroshnichenko, V. Ruzhichd, and V. San'kov (1997). Paleostress reconstructions and geodynamics of the Baikal region, central Asia. Part II: Cenozoic rifting, in *Structural Controls on Sedimentary Basin Formation*, S. Cloetingh, M. Fernandez, J. A. Munoz, W. Sassi, and F. Horvath (Editors), special issue, *Tectonophysics* **282,** 1–38.

Doutsos, T., and D. J. W. Piper (1990). Listric faulting, sedimentation and morphological evolution of the Quaternary eastern Corinth rift, Greece: First stages of continental rifting, *Bull. Seismol. Soc. Am.* **102,** 812–829.

Durand, V., M. Bouchon, N. Thedoulidis, and D. Marsan (2013). Interplay between slow deformation and large earthquakes in Greece, *Eos Trans. AGU* (Fall Meet.), 9–13 December 2013, San Francisco, California, Abstract 1801476.

Feng, L., A. N. Newman, G. T. Farmer, P. Psimoulis, and S. Stiros (2010). Energetic rupture, coseismic and post-seismic response of the 2008 M_w 6.4 Achaia-Elia earthquake in northwestern Peloponnese, Greece: An indicator of an immature transform fault zone, *Geophys. J. Int* **183,** 103–110.

Flotté, N., D. Sorel, C. Müller, and J. Tensi (2005). Along strike changes in the structural evolution over abrittle detachment fault: Example of Pleistocene Corinth-Patras rift (Greece), *Tectonophysics* **403,** 77–94.

Freed, A. M. (2005). Earthquake triggering by dynamic, static and post-seismic stress transfer, *Annu. Rev. Earth Planet. Sci.* **33,** 335–367.

Gallousi, C., and I. K. Koukouvelas (2007). Quantifying geomorphic evolution of earthquake triggered landslides and their relation to active normal faults. An example from the Gulf of Corinth, Greece, *Tectonophysics* **440,** no. 1–4, 85–104, doi: 10.1016/j.tecto.2007.02.009.

Ganas, A., E. Serpelloni, G. Drakatos, M. Kolligri, I. Adamis, Ch. Tsimi, and E. Batsi (2009). The M_w 6.4 SW-Achaia (western Greece) earthquake of 8 June 2008: Seismological, filed, GPS observations and stress modeling, *J. Earthq. Eng.* **13,** no. 8, 1101–1124.

Hardebeck, J. L., and A. J. Michael (2004). Stress orientations at intermediate angles to the San Andreas fault, California, *J. Geophys. Res.* **109,** no. B11303 doi: 10.1029/2004JB003239.

Hardebeck, J. L., J. J. Nazareth, and E. Hauksson (1998). The static stress change triggering model: Constraints from two southern California earthquake sequences, *J. Geophys. Res.* **103,** 24,427–24,437.

Heidbach, O., M. Tingay, A. Barth, J. Reinecker, D. Kurfeß, and B. Muller (2010). Global crustal stress pattern based on the World Stress Map database release 2008, *Tectonophysics* **482,** 3–15.

Kamberis, E., S. Sotiropoulos, O. Aximniotou, S. Tsaila-Monopoli, and C. Ioakim (2000). Late Cenozoic deformation of the Gavrovo and Ioanian zones, *Ann. Geophys.* **43,** no. 5.

Kapetanidis, V. (2007). Study of swarms in western Corinth gulf using cross-correlation and similarity: Redetermination of seismic parameters, *M.Sc. Thesis*, National and Kapodistrian University of Athens, 312 pp.

Kapetanidis, V., A. Agalos, A. Moshou, G. Kaviris, A. Karakonstantis, P. Papadimitriou, and K. Makropoulos (2008). Preliminary Results from the Study of a Seismic Swarm Occurred in February 2008 in NW Peloponnesus, Greece, *31st General Assembly of the European Seismological Commission, Heraklio, Greece*, available at http://www.geophysics.geol.uoa.gr/papers/ESC2008/kapetanidis_ESC2008_poster.pdf (last accessed February 2013).

King, G. C. P., R. S. Stein, and J. Lin (1994). Static stress changes and the triggering of earthquakes, *Bull. Seismol. Soc. Am.* **84,** 935–953.

Kissling, E., W. L. Ellsworth, D. Eberhart-Phillips, and U. Kradolfer (1994). Initial reference models in local earthquake tomography, *J. Geophys. Res.* **99,** no. B10, 19,635–19,646.

Konstantinou, K. I., C. P. Evangelidis, and N. S. Melis (2011). The 8 June 2008 M_w 6.4 earthquake in northwest Peloponnese, western Greece: A case of fault reactivation in an overpressured lower crust? *Bull. Seismol. Soc. Am.* **101,** no. 1, 438–445.

Konstantinou, K. I., N. S. Melis, S.-J. Lee, C. P. Evangelidis, and K. Boukourtas (2009). Rupture process and aftershocks relocation of the 8 June 2008 M_w 6.4 earthquake in northwest Peloponnese, western Greece, *Bull. Seismol. Soc. Am.* **99,** no. 6, 3374–3389.

Latorre, D., J. Virieux, T. Monfret, V. Monteiller, T. Vanorio, J. L. Got, and H. Lyon-Caen (2004). A new seismic tomography of Aigion area (Gulf of Corinth, Greece) from the 1991 data set, *Geophys. J. Int.* **159,** no. 3, 1013–1031, doi: 10.1111/j.1365-246X.2004.02412.x.

Lin, J., and R. S. Stein (2004). Stress triggering in thrust and subduction earthquakes, and stress interaction between the southern San Andreas and nearby thrust and strike-slip faults, *J. Geophys. Res.* **109,** no. B02303, doi: 10.1029/2003JB002607.

Makris, J. (1978). The crust and upper mantle of the Aegean region from deep seismic soundings, *Tectonophysics* **46,** 269–284.

Matthews, M. V., and P. A. Reasenberg (1988). Statistical methods for investigating quiescence and other temporal seismicity patterns, *Pure Appl. Geophys.* **126,** 357–372.

Melis, N., G. Tselentis, and E. Sokos (1994). The Pyrgos (March 26, 1993; $M_s = 5.2$) earthquake sequence as it was recorded by the Patras Seismic Network, *Bull. Geol. Soc. Greece.* **30,** no. 5, 175–180.

Orfanogiannaki, K., and G. A. Papadopoulos (2004). Seismicity criteria for the real-time identification of foreshocks in the Corinth gulf, *Bull. Geol. Soc. Greece* **XXXVI,** 1451–1456.

Pacchiani, F., and H. Lyon-Caen (2010). Geometry and spatio-temporal evolution of the 2001 Agios Ioanis earthquake swarm (Corinth rift, Greece), *Geophys. J. Int.* **180,** no. 1, 59–72, doi: 10.1111/j.1365-246X.2009.04409.x.

Papadopoulos, G. A., V. Karastathis, C. Kontoes, M. Charalambakis, A. Fokaefs, and I. Papoutsis (2010). Crustal deformation associated with east Mediterranean strike-slip earthquakes: The 8 June 2008 Movri (NW Peloponnese), Greece, earthquake (M_w 6.4), *Tectonophysics* **492,** 201–212.

Papazachos, B. C., and C. B. Papazachou (1989). *The Earthquakes of Greece*, Ziti Publ., Thessaloniki, Greece, 356 pp. (in Greek).

Papazachos, B. C., P. E. Comninakis, G. F. Karakaisis, B. G. Karakostas, Ch. A. Papaioannou, C. B. Papazachos, and E. M. Scordilis (2000). *A Catalogue of Earthquakes in Greece and Surrounding Area for the Period 550BC–1999*, Vol. 1, Publ. Geophys. Laboratory, University of Thessaloniki, Greece, 333 pp.

Parsons, T. (2002). Nearly frictionless faulting from unclamping in long-term interaction models, *Geology* **30,** 1063–1066.

Perfettini, H., R. S. Stein, R. Simpson, and M. Cocco (1999). Stress transfer by the 1988–1989 $M = 5.3$ and 5.4 Lake Elsman foreshocks to the Loma Prieta fault: Unclamping at the site of peak mainshock slip, *J. Geophys. Res.* **104,** no. B9, 20,169–20,182, doi: 10.1029/1999JB900092.

Reasenberg, P. A., and R. W. Simpson (1992). Response of regional seismicity to the static stress change produced by the Loma Prieta earthquake, *Science* **255,** 1687–1690

Rice, J. R. (1992). Fault stress states, pore pressure distributions, and the weakness of the San Andreas fault, in *Fault Mechanics and Transport Properties of Rocks: A Festschrift in Honor of W. F. Brace*, B. Evans and T. Wong (Editors), Academic Press, San Diego, California, 475–503.

Rigo, A., H. Lyon-Caen, R. Armijo, A. Deschamps, D. Hatzfeld, K. Makropoulos, P. Papadimitriou, and I. Kassaras (1996). A microseismic study in the western part of the Gulf of Corinth (Greece): Implications for large-scale normal faulting mechanisms, *Geophys. J. Int.* **126,** no. 3, 663–688.

Roberts, G. P., and I. Koukouvelas (1996). Structural and seismological segmentation of the Gulf of Corinth fault system: Implications for models of fault growth, *Ann. Geophys.* **39,** no. 3, 619–646.

Sachpazi, M., A. Hirn, C. Clement, F. Haslinger, E. Kissling, and P. Charvis (2000). Western Hellenic subduction and Cephalonia transform: Local earthquakes and plate transport strain, *Tectonophysics* **319,** 301–319.

Serpelloni, E., M. Anzidei, P. Baldi, G. Casula, and A. Galvani (2005). Crustal velocity and strain-rate fields in Italy and surrounding regions: New results from the analysis of permanent and non-permanent GPS networks, *Geophys. J. Int.* **161,** 861–880, doi: 10.1111/j.1365-246X.2005.02618.x.

Sokos, E., J. Zahradnik, A. Kiratzi, J. Jansky, F. Gallovic, O. Novotny, J. Kostelecký, A. Serpetsidaki, and G.-A. Tselentis (2012). The January 2010 Efpalio earthquake sequence in the western Corinth gulf (Greece), *Tectonophysics* **530/531,** 229–309.

Vassilakis, E., L. Royden, and D. Papanikolaou (2011). Kinematic links between subduction along the Hellenic trench and extension in the Gulf of Corinth, Greece: A multidisciplinary analysis, *Earth Planet. Sci. Lett.* **303,** nos. 1/2, 108–120, doi: 10.1016/j.epsl.2010.12.054.

Waldhauser, F. (2001). hypoDD: A computer program to compute double-difference earthquake locations, *U.S. Geol. Surv. Open-File Rept. 01-113* Version 1, available at http://geopubs.wr.usgs.gov/open-file/of01-113/ (last accessed February 2013).

Waldhauser, F., and W. L. Ellsworth (2000). A double-difference earthquake location algorithm: Method and application to the northern Hayward fault, California, *Bull. Seismol. Soc. Am.* **90,** 1353–1368.

Wiemer, S. (2001). A software package to analyze seismicity: ZMAP, *Seismol. Res. Lett.* **72,** 373–382.

Wiemer, S., and M. Wyss (2000). Minimum magnitude of complete reporting in earthquake catalogs: Examples from Alaska, the Western United States, and Japan, *Bull. Seismol. Soc. Am.* **90,** 859–869.

Woessner, J., and S. Wiemer (2005). Assessing the quality of earthquake catalogues: Estimating the magnitude of completeness and its uncertainty, *Bull. Seismol. Soc. Am.* **95,** no. 2, 684–698.

Zhang, Z., J. Y. Chen, and J. Lin (2008). Stress interactions between normal faults and adjacent strike slip faults of 1997 Jiashi earthquake swarm, *Sci. China Earth Sci.* **51,** no. 3, 431–440.

Zoback, M. L., and M. Magee (1991). Stress magnitudes in the crust: Constraints from stress orientation and relative magnitude data, *Phil. Trans. Roy. Soc. London. A* **337,** 181–194.

U.S. Geological Survey
345 Middlefield Road
Menlo Park, California 94025
segou@unice.geoazur.fr
ellsworth@usgs.gov
tparsons@usgs.gov

Manuscript received 31 May 2013;
Published Online 22 July 2014